Available online at www.sciencedirect.com
ScienceDirect
Theoretical Population Biology 72 (2007) 121–135
Theoretical Population Biology
www.elsevier.com/locate/tpb

Fixation in haploid populations exhibiting density dependence I: The non-neutral case

Todd L. Parsons[a,*], Christopher Quince[b]

[a]Department of Mathematics, University of Toronto, 40 St. George Street, Toronto, Ont., Canada M5S 2E4
[b]Department of Ecology and Evolutionary Biology, 25 Harbord Street, University of Toronto, Toronto, Ont., Canada M5S 3G5

Received 30 September 2006
Available online 15 December 2006

Abstract

We extend the one-locus two allele Moran model of fixation in a haploid population to the case where the total size of the population is not fixed. The model is defined as a two-dimensional *birth-and-death* process for allele number. Changes in allele number occur through density-independent death events and birth events whose per capita rate decreases linearly with the total population density. Uniquely for models of this type, the latter is determined by these same birth-and-death events. This provides a framework for investigating both the effects of fluctuation in total population number through demographic stochasticity, and deterministic density-dependent changes in mean density, on allele fixation. We analyze this model using a combination of asymptotic analytic approximations supported by numerics. We find that for advantageous mutants demographic stochasticity of the resident population does not affect the fixation probability, but that deterministic changes in total density do. In contrast, for deleterious mutants, the fixation probability increases with increasing resident population fluctuation size, but is relatively insensitive to initial density. These phenomena cannot be described by simply using a harmonic mean effective population size.

Keywords: Fixation; Density dependent; Logistic; Stochastic; Asymptotic; Allele; Competition

1. Introduction

For almost a century, there has been a sustained interest in determining the fixation probability of a new mutant allele, and thereby obtaining estimates of the rate of evolutionary change. A number of models have been proposed, relying on a number of simplifying assumptions to retain analytical tractability. The earliest of these models assumed a resident population of fixed size and neglected the effects of interaction between individuals, defining fixation as non-extinction (and thus exponential population growth) for the mutant type (Fisher, 1922; Haldane, 1927). Later, the Wright–Fisher model (Fisher, 1958; Wright, 1931), from which fixation probabilities were determined using a diffusion approximation by Kimura (1957, 1962), and the Moran model (Moran, 1958), would incorporate density dependence by assuming fixed population sizes. Other authors have considered the effects of changing population sizes by assuming some form of deterministic population growth (Ewens, 1967; Kimura and Ohta, 1974; Otto and Whitlock, 1997).

There is an equally long tradition in ecology of attempting to determine the dynamics of population growth from the interactions of individuals. In particular, logistic and Lotka–Volterra models and related stochastic models, e.g., Nisbet and Gurney (1982), Nåsell (2001), have become standard tools in understanding the effects of density dependence on dynamic, interacting populations subject to endogenous and exogenous fluctuations. In what follows, we present a model that unifies these two threads, allowing us to analyze analytically and numerically fixation in stochastically varying populations. We are thus able to ascertain the impact of population growth and decline and demographic stochasticity on fixation, when those population dynamics are derived from the interactions of individuals, rather than assumed a priori.

*Corresponding author.
E-mail addresses: parsons@math.toronto.edu (T.L. Parsons), quince@zoo.utoronto.ca (C. Quince).

0040-5809/$ - see front matter © 2006 Elsevier Inc. All rights reserved.
doi:10.1016/j.tpb.2006.11.004

We consider a haploid model of two types with discrete individuals but continuous time. These types can be viewed as possessing two different alleles. Death occurs at density-independent per capita rates, but birth rates are linearly decreasing functions of the total population size. Both types therefore undergo logistic growth. The model can be viewed as either an extension of the Moran model of population genetics to the case where total population size is allowed to vary, or an extension of a version of the stochastic logistic process to two competing types. The model therefore has relevance to population genetics as a model of allele fixation, or to population biology as a model of competing species.

We begin by defining our model of density-dependent allele fixation. This model is then examined directly by exact numerical methods, and systematically approximated via asymptotic methods for which the error can be quantified, thereby allowing a coherent framework for the analysis of fixation probabilities. This framework is used to examine the two cases of fixation of advantageous and deleterious mutants. Finally, we present some numerical results on fixation times. In this paper we do not treat the case when the alleles have equal carrying capacities. We consider this case in a subsequent paper (Parsons and Quince, submitted).

2. A model of allele fixation with density-dependent population dynamics

We consider a haploid population comprised of two types, extending the Moran model (Moran, 1958), by relaxing the assumption of a fixed population number. Instead, we allow the total population number to change with the same birth-and-death events that determine allele fixation. This will allow us to investigate the effect of changes in the total population size on allele fixation.

We consider an environment with K sites, where each site can be occupied by at most one individual. This individual can be of either type $\mathcal{X}$, if they possess the A_X allele, or type $\mathcal{Y}$, if they possess the A_Y allele. Death is assumed to occur at type specific per capita rates, μ_x and μ_y, for individuals of type $\mathcal{X}$ and type $\mathcal{Y}$, respectively. Death is therefore density independent. Each individual of type $\mathcal{X}$ or type $\mathcal{Y}$ attempts to reproduce at type specific rates λ_x and λ_y. When an attempted reproduction event occurs, a site is chosen at random. If that site is empty, then a new individual of the parent's type is placed in it. If that site is occupied, reproduction fails. Reproduction is therefore density dependent. This model is an extension of a stochastic model of logistic growth, e.g., Nisbet and Gurney (1982), Nåsell (2001), Newman et al. (2004), to two competing types. The single-type case has also been used to model population dynamics in a patchy environment (Gurney and Nisbet, 1978).

We model this system via a Markov chain on $\{(X, Y)|X + Y \leqslant K\} \subset \mathbb{Z}^2$ with transition rates, probabilities per unit time, as given in Table 1.

Table 1
Transition rates

Transition $(X, Y) \to (X', Y')$	Rate $W_{(X',Y'),(X,Y)}$
$(X, Y) \to (X + 1, Y)$	$\lambda_x X\left(1 - \frac{X+Y}{K}\right)$
$(X, Y) \to (X, Y + 1)$	$\lambda_y Y\left(1 - \frac{X+Y}{K}\right)$
$(X, Y) \to (X - 1, Y)$	$\mu_x X$
$(X, Y) \to (X, Y - 1)$	$\mu_y Y$

The probabilities that at time t we are in a state with X-type $\mathcal{X}$ individuals and Y-type $\mathcal{Y}$ individuals, $P_{(X,Y)}(t)$, are described by a master equation (van Kampen, 1992), of the form:

$$\frac{dP_{(X,Y)}}{dt} = \sum_{(X',Y')} W_{(X,Y),(X',Y')} P_{(X',Y')}(t) - \sum_{(X'',Y'')} W_{(X'',Y''),(X,Y)} P_{(X,Y)}(t). \quad (1)$$

The $W_{(X,Y),(X',Y')}$ are the transition rates from the state (X', Y') to (X, Y).

We show below that, in the deterministic limit of zero population size, the type with the larger ratio of birth to death rates will come to comprise the entire population. This ratio is therefore a good definition of fitness for our model. We assume that for both types it is greater than one, $\lambda_x > \mu_x$ and $\lambda_y > \mu_y$. This ensures that both types are capable of increasing when rare. The relative fitness of the two types, $v = \lambda_x \mu_y / \mu_x \lambda_y$, will also prove to be a useful quantity.

This model is intended to provide a simple description of haploid population genetics for which births and deaths are represented by processes operating at the level of individuals. It is not the most general model of two types with birth rates that are a linear function of population density—that would require six rather than five parameters—since it assumes that competition decreases the growth rates of both types by the same proportion.

The model can also be viewed as an extension of a fixed population size stochastic SIS process (Jacquez and Simon, 1993), to two infection types that are competing for the same pool of susceptible individuals. The number of susceptible individuals is the number of empty sites $K - X + Y$, and infection rates correspond to the birth rates λ_x and λ_y, and recovery rates to the death rates μ_x and μ_y.

The appeal of this model is that it allows us to study the interaction between allele fixation and discrete density-dependent population dynamics in a reasonably tractable framework. It is the aim of this study to determine as much as possible about fixation in this model. We shall do this using a combination of direct numerical calculations and analytic asymptotic approximations. In this paper we restrict ourselves to the case where the two types have

different fitnesses, so $v \neq 1$. We will consider the case $v = 1$ in a forthcoming paper (Parsons and Quince, submitted).

$$\pi_{(X,Y)} = \frac{\mu_x X \pi_{(X-1,Y)} + \lambda_x X(1 - N/K)\pi_{(X+1,Y)} + \mu_y Y \pi_{(X,Y-1)} + \lambda_y Y(1 - N/K)\pi_{(X,Y+1)}}{\mu_x X + \lambda_x X(1 - N/K) + \mu_y Y + \lambda_y Y(1 - N/K)} \tag{3}$$

It is useful here to introduce some terminology. We generally assume that type $\mathcal{X}$ has a lower fitness than type $\mathcal{Y}$, $v < 1$. If we use the term mutant for one type, then this implies that its population size is considerably smaller than the other type, which we refer to as the resident.

It will also prove useful to define the fixed population size Moran model equivalent to the density-dependent model we have described (Moran, 1958). This corresponds to the case where the two types die at rates μ_x and μ_y as above, but the population size is kept fixed by assuming that each death event is immediately followed by the production of a new individual whose parent is chosen randomly from those present before the death event but weighted by factors λ_x and λ_y. This is a one-dimensional *birth-and-death process*, e.g., van Kampen (1992), because the state of the system is completely described by the number of type $\mathcal{X}$ individuals, therefore it is a standard result (Ewens, 1979), that the probability that type $\mathcal{X}$ fixes starting from M individuals is

$$\pi_M = \frac{v^N - v^{N-M}}{v^N - 1}, \tag{2}$$

where $v = \mu_y \lambda_x / \mu_x \lambda_y$ is the relative fitness of type $\mathcal{X}$ to type $\mathcal{Y}$.

For the density-dependent model, which is a two-dimensional birth-and-death process, no such simple result exists for the fixation probability. We therefore begin in Section 3 by introducing numerical methods that can be used to determine the fixation probability. In Section 4, we then describe the derivation of the asymptotic approximation to the fixation probability of the deleterious type $\mathcal{X}$. This approximation becomes exact for all initial densities of type $\mathcal{X}$ and $\mathcal{Y}$ in the limit $K \to \infty$. However, for intermediate K values, it is only accurate for relatively small initial densities of the advantageous type $\mathcal{Y}$. We therefore use one minus the asymptotic approximation to investigate fixation of advantageous type $\mathcal{Y}$ mutants (Section 5.1). For deleterious mutants we use numerical results (Section 5.2). Finally, we numerically determine mean fixation times for both deleterious and advantageous mutants in Section 6.

3. Numerical evaluation of the fixation probability

We will denote the probability that type $\mathcal{X}$ fixes starting from a state (X, Y) by $\pi_{(X,Y)}$. This is the probability that a state on the $Y = 0$ boundary is reached before a state with $X = 0$. These boundaries are absorbing: once $X = 0$ or $Y = 0$, it will remain zero. By considering the probability of transitions to neighboring states, it can be shown that the fixation probability obeys:

for all $X > 0$, $Y > 0$ with $X + Y \leqslant K$. These equations have boundary conditions $\pi_{(0,Y)} = 0$ and $\pi_{(X,0)} = 1$. In the next section, when we derive analytic approximations to these equations, we study their continuous equivalent (Eq. (4)).

In general we cannot solve Eq. (3), but note that when $\mu_x = \mu_y$ and $\lambda_x = \lambda_y$, $\pi_{(X,Y)} = X/N$, as would be expected from symmetry. We can, however, evaluate the relations numerically by using Eq. (3) to obtain a matrix equation for the fixation probabilities (Stewart, 1994). Using a sparse matrix library, UMFPACK (Davis, 2004), it was possible to directly compute fixation probabilities for reasonably large systems ($K \approx 1000$) on a computer equipped with a typical 1 GHz processor. These system sizes are large enough for stable populations to form, but small enough so that demographic stochasticity is still important. The numerical component of our study will focus on systems of this size. It is also possible to calculate mean fixation times in a similar way.

In Fig. 1 we show an example illustrating the dependence of the fixation probability on the initial densities for the

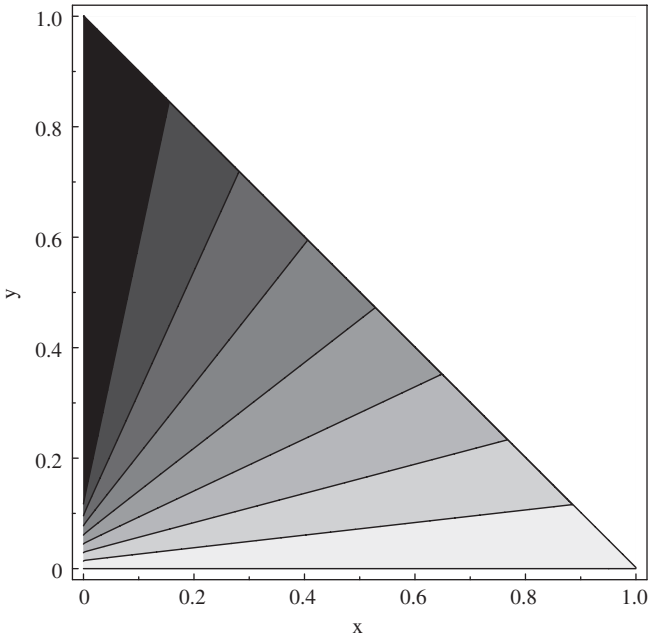

Fig. 1. The log of the fixation probability $\log(\pi_{(X,Y)})$ as a function of initial-type $\mathcal{X}$ ($x = X/K$) and type $\mathcal{Y}$ ($y = Y/K$) densities. The figure is a contour plot of exact numerical evaluations for $\lambda_y = 1.0$, $\mu_y = 0.5$, $\lambda_x = 1.0$, $\mu_x = 0.6$, and $K = 1000$. Dark areas correspond to reduced fixation probability. The contour closest to the x-axis is -10, and after that they decrease in increments of 10, so that the last contour in the darkest region of the graph is -70. Note that probabilities are only defined for $x + y \leqslant 1$.

case of a deleterious type $\mathcal{X}$. It is clear from this figure that increasing the initial density of $\mathcal{X}$, or decreasing the initial density of $\mathcal{Y}$, increases the fixation probability of $\mathcal{X}$. This is what we would expect.

4. Asymptotic estimates for the fixation probability

The discrete master equation (1) is analytically intractable. To make progress we convert it into a continuous PDE. We begin by introducing rescaled variables $x = X/K$ and $y = Y/K$ corresponding to the densities of type $\mathcal{X}$ and type $\mathcal{Y}$, respectively. As K becomes large, the step size for the one-step process becomes vanishingly small. We may thus make a diffusion approximation, using a Taylor expansion to approximate the master equation (Eq. (1)) by a Fokker–Planck equation, e.g., van Kampen (1992): writing p for the probability of having population densities x and y at time t,

$$\frac{\partial p}{\partial t} = -\frac{\partial}{\partial x}[\lambda_x x(1-x-y)-\mu_x x]p - \frac{\partial}{\partial y}[\lambda_y y(1-x-y)-\mu_y y]p + \frac{1}{2K}\left\{\frac{\partial^2}{\partial x^2}[\lambda_x x(1-x-y)+\mu_x x]p + \frac{\partial^2}{\partial y^2}[\lambda_y y(1-x-y)+\mu_y y]p\right\},$$

p is defined on the first quadrant, Ω, with boundary

$$\partial\Omega = \{(x,y)|x=0 \text{ or } y=0\}.$$

This is a singular diffusion with characteristic boundary (Matkowsky et al., 1983).

We are interested in the probability that the deleterious type $\mathcal{X}$ fixes. Let

$$\partial\Omega_1 = \{(x,y)|y=0, x>0\} \quad \text{and}$$
$$\partial\Omega_0 = \{(x,y)|x=0, y\geqslant 0\}.$$

Then the probability of fixation from initial population densities (x,y) is equal to the probability of eventual exit through $\partial\Omega_1$. We denote this probability by $\pi(x,y)$. Then, it is a well-known result, e.g., Gardiner (2004), that π satisfies the boundary value problem

$$[\lambda_x x(1-x-y)-\mu_x x]\frac{\partial\pi}{\partial x} + [\lambda_y y(1-x-y)-\mu_y y]\frac{\partial\pi}{\partial y} + \frac{1}{2K}\left\{[\lambda_x x(1-x-y)+\mu_x x]\frac{\partial^2\pi}{\partial x^2} + [\lambda_y y(1-x-y)+\mu_y y]\frac{\partial^2\pi}{\partial y^2}\right\} = 0,$$

$$\pi(x,0) = 1,$$

$$\pi(0,y) = 0. \tag{4}$$

It is useful to introduce a change of coordinates

$$u = x+y, \quad v = \frac{x}{x+y},$$

with u the total population size, and v the frequency of type $\mathcal{X}$. This new coordinate system is more commonly used when looking at fixation probabilities. Moreover, outside of a neighborhood of the origin, we found that asymptotics obtained in the new coordinate system were more accurate for intermediate K than asymptotics obtained from the untransformed equations. This was determined by comparison to the exact numerical computations.

Near $(0,0)$, the transformation $(x,y)\to(u,v)$ is not bijective; we will examine the behavior near this point later in the text.

In the new coordinate system, $(0,0)$ is mapped to the line $u=0$, $\partial\Omega_1$ is mapped to the line $v=1$, and $\partial\Omega_0 - \{(0,0)\}$ is mapped to the line $v=0$. In what follows, we will use $\partial\Omega_0$ and $\partial\Omega_1$ to refer to their images in the uv-plane.

In terms of u and v, the boundary value problem (4) becomes

$$[(\lambda_y(1-v)+\lambda_x v)\mu(1-u)-(\mu_y(1-v)+\mu_x v)u]\frac{\partial\pi}{\partial u} + v(1-v)\left(1+\frac{1}{uK}\right)[(\lambda_x-\lambda_y)(1-u)-(\mu_x-\mu_y)]\frac{\partial\pi}{\partial v} + \frac{1}{2K}\left\{[\lambda_y(1-v)+\lambda_x v)u(1-u)+(\mu_y(1-v)+\mu_x v)u]\frac{\partial^2\pi}{\partial u^2} + 2v(1-v)[(\lambda_x-\lambda_y)(1-u)+(\mu_x-\mu_y)]\frac{\partial\pi}{\partial u\partial v} + \frac{v(1-v)}{u}[\lambda_x(1-u)+\mu_x+(\lambda_x-\lambda_y)v(1-u)+(\mu_x-\mu_y)v]\frac{\partial^2\pi}{\partial v^2}\right\} = 0,$$

$$\pi(0,v) = 0,$$

$$\pi(u,1) = 1,$$

$$\pi(u,0) = 0. \tag{5}$$

We cannot explicitly solve this system, but it is possible to obtain formal asymptotics for large K via singular perturbation methods (Matkowsky et al., 1983; Roozen, 1989; Hinch, 1991; Kevorkian and Cole, 1996; Grasman and van Herwaarden, 1999). In this approach, we use a regular asymptotic series in powers of K to obtain an 'outer approximation' to $\pi(x,y)$ in the interior of Ω. This solution will not be compatible with both boundary conditions, so we will make use of coordinate stretching transformations to obtain compatible 'inner approximations' near $\partial\Omega_1$. In general, we expect inner approximations to be necessary in regions where the derivatives of π change rapidly. As these regions typically occur near the boundaries of the domain, we refer to them as *boundary layers*.

4.1. The outer approximation

We start by looking for a solution of the form

$$\pi(u,v) = \pi_0(u,v) + \pi_1(u,v)K^{-1} + \pi_2(u,v)K^{-2} + \cdots. \tag{6}$$

We will focus our efforts on π_0, which, outside of a neighborhood of $\partial\Omega_1$, will be equal to π in the limit as $K\to\infty$.

Substituting (6) into the backward Fokker–Planck equation (5) and taking the limit as $K\to\infty$, we find that

$$[(\lambda_y(1-v)+\lambda_x v)u(1-u)-(\mu_y(1-v)+\mu_x v)u]\frac{\partial\pi_0}{\partial u} + v(1-v)[(\lambda_x-\lambda_y)(1-u)-(\mu_x-\mu_y)]\frac{\partial\pi_0}{\partial v} = 0. \tag{7}$$

This linear equation describes the deterministic component of the process. We solve it by the method of characteristics: if we introduce a parameter t so that on a characteristic, $u = u(t)$ and $v = v(t)$, then

$$\frac{\partial \pi_0}{\partial t} = \dot{u}(t)\,\frac{\partial \pi_0}{\partial u} + \dot{v}(t)\,\frac{\partial \pi_0}{\partial v},$$

where u and v satisfy the dynamical system

$$\begin{aligned}\dot{u} &= [\lambda_y(1-v) + \lambda_x v]u(1-u) - [\mu_y(1-v) + \mu_x v]u,\\ \dot{v} &= v(1-v)[(\lambda_x - \lambda_y)(1-u) - (\mu_x - \mu_y)].\end{aligned} \tag{8}$$

Then, from (7), $\partial\pi_0/\partial t = 0$, so π_0 is constant along the integral curves of (8). These curves are shown in Fig. 2.

Thus, we see that the deterministic component of the total population growth is logistic, with birth-and-death rates equal to the population average, while the portion of type $\mathcal{X}$ is decreasing if

$$u > 1 - \frac{\mu_x - \mu_y}{\lambda_x - \lambda_y}$$

and increasing otherwise, which can occur if, for example, $1 < \mu_y/\mu_x < \lambda_y/\lambda_x$. When $\lambda_x = \lambda_y$, the deterministic flow in v is strictly towards $v = 0$ and independent of population size, which will lead to a particularly simple expression for the fixation probability for this case.

If $\lambda_x/\mu_x \neq \lambda_y/\mu_y$, then (8) has equilibria at $(\bar{u}_0, 0) = (1 - \mu_y/\lambda_y, 0)$ and $(\bar{u}_1, 1) = (1 - \mu_x/\lambda_x, 1)$. If $\lambda_x/\mu_x < \lambda_y/\mu_y$, then $(\bar{u}_0, 0)$ is stable and $(\bar{u}_1, 1)$ is unstable, while the opposite is true when $\lambda_x/\mu_x > \lambda_y/\mu_y$.

If $\lambda_x/\mu_x = \lambda_y/\mu_y$ then the line $u = 1 - \mu_x/\lambda_x = 1 - \mu_u/\lambda_y$ is a center manifold and attractor for (8).

The different underlying deterministic dynamics require us to consider these two cases separately. Here, we will focus on the case where $\lambda_x/\mu_x < \lambda_y/\mu_y$, and present our analysis of the case $\lambda_x/\mu_x = \lambda_y/\mu_y$ in a future work (Parsons and Quince, submitted).

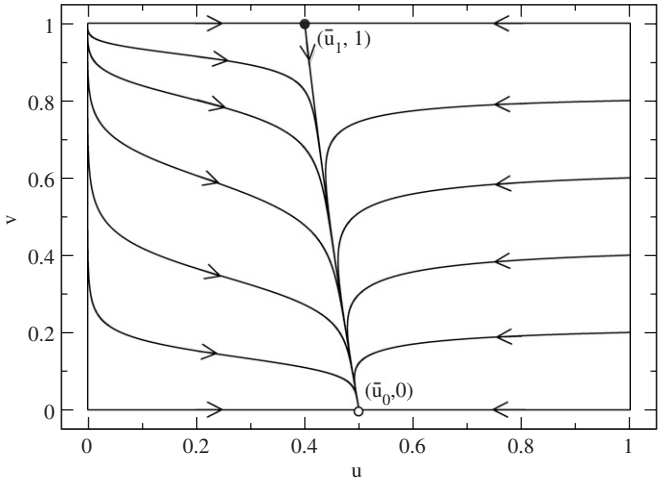

Fig. 2. Phase diagram in the uv-plane for the ODEs of Eq. (8) when $\lambda_x/\mu_x < \lambda_y/\mu_y$. The solid lines show flows with arrows giving directions. The unstable node $(\bar{u_1}, 1)$ is shown as a black circle and the stable node $(\bar{u_0}, 0)$ as an open circle. The actual parameters used were $\lambda_y = 1.0$, $\mu_y = 0.5$, $\lambda_x = 1.0$, $\mu_x = 0.6$. The gray vertical lines merely delimit the region $u, v \leqslant 1$.

When $\lambda_x/\mu_x < \lambda_y/\mu_y$, any flow beginning at a point $(u, v) \notin \partial\Omega_1$ will eventually reach the stable equilibrium at $(\bar{u}_0, 0)$. Since π is constant on flows, in the limit as $K \to \infty$, $\pi_0(u, v) \equiv \pi(\bar{u}_0, 0) = 0$ on the interior of Ω.

4.2. The inner approximation

The outer approximation is not consistent with the boundary condition $\pi(u, 1) = 1$, so we will look for a boundary layer solution $\tilde{\pi}$ along $\partial\Omega_1$. This boundary layer arises because the fixation probability of $\mathcal{X}$ will be vanishing small, except when the proportion of type $\mathcal{Y}$ is small, but will grow rapidly to 1 on the boundary.

Moreover, since the dynamical system (8) has a critical point at $(\bar{u}_1, 1)$ that is attracting on $\partial\Omega_1$, the probability of fixation of type $\mathcal{X}$ will increase rapidly in a neighborhood of this point. We thus also look at a subboundary layer solution $\hat{\pi}$ near $(\bar{u}_1, 1)$. By matching these solutions with the outer approximation, we obtain an asymptotic for π that will have error of order $O(K^{-1})$ except in the vicinity of the origin.

In Appendix A we derive the subboundary layer solution near $(\bar{u}_1, 1)$. This solution, Eq. (A.2), rewritten in terms of u and v is

$$\hat{\pi}(u, v) = \exp\left(-\bar{u}_1 \frac{(1-v)}{(1+v)} K(1-v)\right). \tag{9}$$

where $\nu = \lambda_x\mu_y/\lambda_y\mu_x$ is the relative fitness of the invading type.

In Appendix B we then derive the full boundary layer solution, $\tilde{\pi}$, along $\partial\Omega_1$. This is determined as Eq. (B.2):

$$\tilde{\pi}(u, v) = e^{-K(1-v)/\Phi(u)}, \tag{10}$$

where for consistency with $\hat{\pi}$:

$$\lim_{u \to \bar{u}_1} \Phi(u) = \frac{1+\nu}{2\bar{u}_1(1-\nu)}. \tag{11}$$

The factor $\Phi(u)$ is in the general case determined by the integral, Eq. (B.5), from which we see that it is always positive and strictly increasing. In the special case where $\lambda_x = \lambda_y = \lambda$, this integral has a simple closed form:

$$\Phi(u) = \frac{\lambda + \mu_y}{2(\lambda - \mu_y)}\,\frac{1}{u} + \frac{\lambda\mu_y}{(\lambda - \mu_y)(\mu_x - \mu_y)}. \tag{12}$$

4.2.1. Comparison to numerical calculations

This asymptotic analytic expression for the fixation probability becomes exact only in the limit of large K, but it should be a good approximation for intermediate values of K. We investigate the accuracy of the approximation for $K = 1000$, and how the error depends on the initial densities, using the numerical methods described in Section 3. These are accurate to machine precision.

The asymptotic approximation, Eq. (10), for the fixation probability of type $\mathcal{X}$, when type $\mathcal{X}$ has a lower fitness than $\mathcal{Y}$, $\lambda_x/\mu_x < \lambda_y/\mu_y$, applies when we are not too close to the

origin. Eq. (10) predicts that the fixation probability should be an exponentially decaying function of the initial proportion of type $\mathcal{Y}$. The function $\Phi(u)$ is positive and depends on the initial population density $u = x + y$, through Eq. (B.5).

This exponential approximation has an error of order K^{-1}. Consequently, it is accurate whenever the fixation probability is sufficiently large. This is illustrated in Fig. 3 where we show a contour plot of the absolute proportional error in this approximation as compared to the numerical calculations as a function of the initial densities x and y. The approximation works well near the $y = 0$ axis, but breaks down near the $x = 0$ axis because the fixation probability there is extremely small. It is also not very effective near the origin because of the non-bijective nature of the (u, v) transformation at that point.

4.3. Behavior near the origin

Near the origin it is more appropriate to use the untransformed densities (x, y) rather than (u, v) coordinates. Using these variables in Appendix C we derive a corner layer solution to the fixation probability:

$$2\int_0^1 \left(1 - e^{-2\frac{\lambda_x-\mu_x}{\lambda_x+\mu_x}\frac{Kx}{1-(1-w)^{\frac{\lambda_x-\mu_x}{\lambda_y-\mu_y}}}}\right)\frac{\lambda_y-\mu_y}{\lambda_y+\mu_y}\frac{Ky}{w^2}e^{-2\frac{\lambda_y-\mu_y}{\lambda_y+\mu_y}\frac{Ky}{w}}\,du. \tag{13}$$

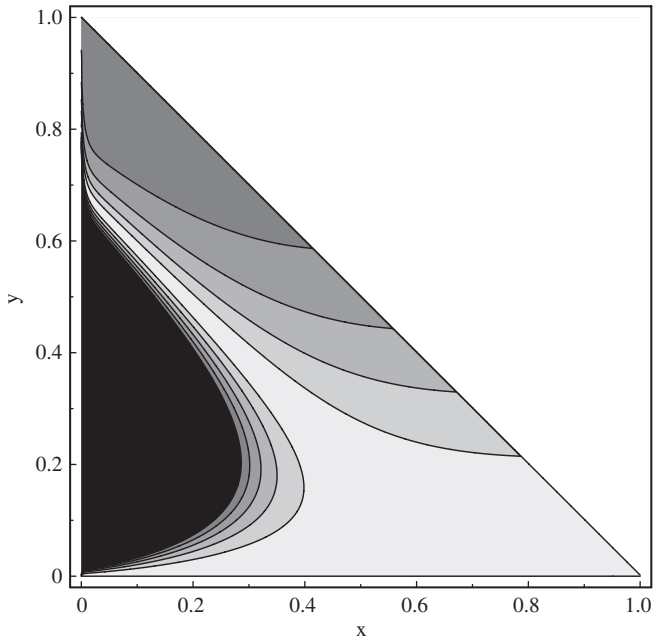

Fig. 3. The proportional absolute error, $|\tilde{\pi}(x, y) - \pi_{(X,Y)}|/\pi_{(X,Y)}$, in the asymptotic approximation to the fixation probability (10), as a function of initial density of type $\mathcal{X}$, x and initial density of type $\mathcal{Y}$, y. The figure is a contour plot for parameter values $\lambda_y = 1.0$, $\mu_y = 0.5$, $\lambda_x = 1.0$, $\mu_x = 0.6$ and $K = 1000$. Dark areas correspond to increased error. The first contour represents 20% error, and after that they increase in increments of 20%. Therefore, the lightest region of the graph corresponds to errors less than 20%, and the darkest region errors greater than 100%. Note that probabilities are only defined for $x + y \leqslant 1$.

This is the probability that type Y becomes extinct at some time at which the number of individuals of type X is nonzero, obtained from diffusion approximations to two density-independent birth-and-death processes with birth rates λ_x and λ_y and death rates μ_x and μ_y.

To avoid ambiguity in what constitutes "near the origin", in Appendix D, we combine the near-origin solution with the interior and boundary layer solutions to obtain a single solution valid over all of Ω,

$$\pi(x, y) = e^{-\frac{Ky}{(x+y)\Phi(x+y)}} - 2\int_0^1 \frac{\lambda_y-\mu_y}{\lambda_y+\mu_y}\frac{Ky}{w^2}e^{-2\frac{\lambda_x-\mu_x}{\lambda_x+\mu_x}\frac{Kx}{1-(1-w)^{\frac{\lambda_x-\mu_x}{\lambda_y-\mu_y}}}-2\frac{\lambda_y-\mu_y}{\lambda_y+\mu_y}\frac{Ky}{w}}\,dw.$$

5. Fixation of mutants

We now apply these results to the case where one type starts with a small population size relative to the other type i.e. a mutant invading a resident population. We will consider the cases of an advantageous and a deleterious mutant separately. In either case prior to the invasion of the mutant the resident population dynamics are described by a stochastic version of the familiar logistic equation of ecology (Nisbet and Gurney, 1982). From Eq. (8) we see that if one type comprises the entire population ($v = 0$ or 1) then in the deterministic limit, $K \to \infty$, the population density $u = N/K$ obeys a standard logistic equation:

$$\dot{u} = [\lambda - \mu]u\left(1 - \frac{u}{1 - \mu/\lambda}\right). \tag{14}$$

Since the resident can be of either type, we have dropped the subscripts from the birth-and-death rates.

The above deterministic equation has a stable state at $\bar{u}_* = (1 - \mu/\lambda)$, so that $K(1 - \mu/\lambda)$ is the equilibrium population size, commonly referred to as the 'carrying capacity'. The stochastic process will fluctuate about this population size, but because zero is an absorbing state, it will eventually go extinct. This, however, will take a very long time, so that it is possible to define a quasi-stationary solution to the stochastic process as the distribution of population sizes conditional on extinction not occurring. This distribution can be determined numerically (Nåsell, 2001; Newman et al., 2004), or approximated by linearizing the stochastic process about the demographic equilibrium (Nisbet and Gurney, 1982), a procedure which can be performed in an asymptotically rigorous way using 'van Kampen's system size expansion' (van Kampen, 1992). This approximation predicts a Gaussian quasi-stationary distribution about the demographic equilibrium with expected standard deviation in density:

$$\langle(u - \bar{u}_*)^2\rangle^{0.5} = \sqrt{\frac{\mu}{\lambda}K}. \tag{15}$$

In Fig. 4 we compare this approximation with numerical results for some typical parameter values.

In the following analysis, we consider both advantageous and deleterious mutants invading a resident population

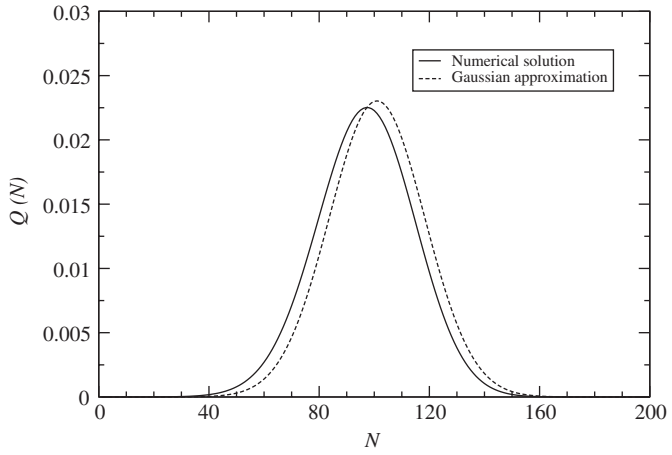

Fig. 4. The quasi-stationary distribution, $Q(N)$, calculated numerically (solid line) and using a Gaussian approximation (dashed line). The results are for $\lambda = 1$, $\mu = 0.75$ and $K = 400$. The deterministic equilibrium occurs at $N^* = 100$ as compared to a mean number averaged over the numerical solution of 96.74. The approximation predicts a standard deviation of 17.32, a numerical calculation gives 17.75.

near its demographic equilibrium, as well as the case when the resident population starts away from equilibrium. The first case allows us to determine the effect of demographic stochasticity in the resident population on mutant fixation, and the second the effect of deterministic changes in population size as the resident returns to equilibrium. However, we should note that in both cases, fixation of the mutant type will be accompanied by a change in the mean population density.

5.1. Fixation of advantageous mutants (type $\mathcal{Y}$)

We showed in Section 4.2.1 that the asymptotic approximation, Eq. (10), holds when the initial density of the fitter type is low, y small, for a system of intermediate size. Therefore, one minus this quantity is an accurate approximation for the fixation probability of an advantageous mutant of type $\mathcal{Y}$ invading a resident population of lower fitness, type $\mathcal{X}$. We will start by considering the case when the total population density is near the demographic equilibrium of the resident, $u \simeq \bar{u}_1$. Then (9) holds, so that the probability of eventual fixation of an advantageous allele, $P(p)$, starting at frequency $p = 1 - v$, is

$$P(p) = 1 - \exp\left(-Np\,\frac{2(1-v)}{1+v}\right), \tag{16}$$

where N is the initial population size $K\bar{u}_1$, and $v = \lambda_x\mu_y/\lambda_y\mu_x$ is the relative fitness of the resident, $v<1$.

The above expression can be compared with Kimura's diffusion approximation for fixation of an allele with selective advantage s, in a haploid population of fixed population size, e.g., Kimura (1957, 1962):

$$P(p) = \frac{1-\exp(-2N_e sp)}{1-\exp(-2N_e s)}.$$

In this equation, N_e is the variance effective population size of the population which has census size N. The variance effective population size is the population size in a Wright–Fisher model that would have the same degree of random genetic drift as the population under consideration (Crow and Morton, 1955; Ewens, 1979). For the fixed size Moran model it is a standard result that this is half the census size, i.e. $N_e = N/2$ (Felsenstein, 1971; Ewens, 1979).

Given our definition of v, $1/v = 1 + s$. When s is small, $2(1-v)/(1+v) \simeq s$. For large population sizes, the denominator of Kimura's approximation will effectively be unity. Therefore, Kimura's expression and that given in Eq. (16) are equivalent if $N_e = N/2$. Thus, the density-dependent model for advantageous alleles invading a resident population near its demographic equilibrium has the same effective population size as the equivalent fixed size Moran model (Ewens, 1979).

For resident populations that start with population density away from $\bar{u}_1$, the effective population size is changed. For a general initial population density we have from (10) that the fixation probability of an advantageous allele is

$$P(p) = 1 - \exp\left(-\frac{Np2(1-v)}{\Psi(u)(1+v)}\right), \tag{17}$$

where N is now the initial population size, Ku, and

$$\Psi(u) = u\Phi(u)/\bar{u}_1\Phi(\bar{u}_1) \tag{18}$$

with $\Phi(u)$ determined by (B.5). This allows us to define a 'Moran effective population size',

$$N_M = \frac{N}{\Psi(u)},$$

the haploid population size in the Moran model that for small s gives the same fixation probability as our density-dependent model. Hereafter, we use this Moran effective population size when we refer to effective population size.

$\Psi(u)$ is positive and increasing for all u, and $\Psi(\bar{u}_1) = 1$. This is illustrated in Fig. 5, where we plot $\Psi(u)$ for four different sets of parameter values for the mutant (type $\mathcal{Y}$). Consequently, the Moran effective population size is equal to N for populations that start near the resident equilibrium $\bar{u}_1$. For populations with initial total density smaller than this, $u<\bar{u}_1$, the effective population size is increased: $N>N_M$. Conversely, when the initial density is greater than the resident equilibrium, the effective population size is reduced, $N<N_M$, as compared to the fixed population size Moran model.

These changes in effective population size with initial density reflect the deterministic flow in u when we start away from the demographic equilibrium, Fig. 2. If u is less than $\bar{u}_1$, the initial growth in population density is accompanied by a rapid decrease in v, the proportion of the inferior resident-type $\mathcal{X}$. This occurs because the inferior type is out-competed in a growing population. This movement away from the $v = 1$ axis ($\partial\Omega_1$) decreases the probability that the resident population will fix against

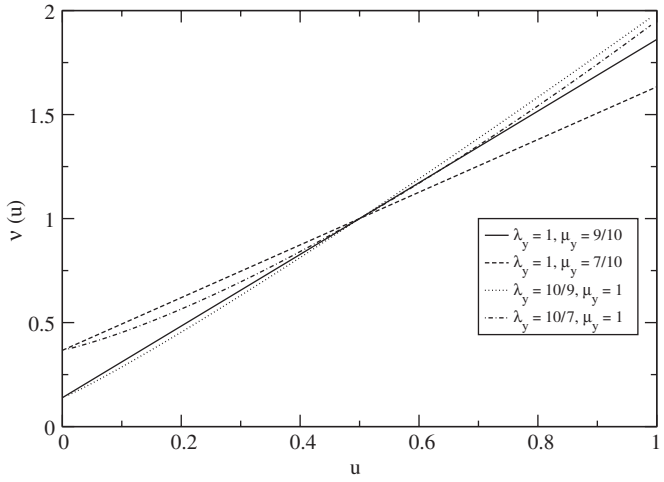

Fig. 5. The factor $\Psi(u)$, which determines the Moran effective population size, $N_M = N/\Psi(u)$, as a function of the initial population density u. Four curves are shown, all with same resident type $\mathcal{X}$ characteristics, $\lambda_x = 1$ and $\mu_x = 0.5$, so that $\bar{u}_1 = 0.5$. In two cases, the mutant type $\mathcal{Y}$ also has $\lambda_y = 1$ and decreased death rates $\mu_y = \frac{9}{10}, \frac{7}{10}$. In the other two cases, $\mu_y = 1$ but the mutant birth rate is increased: $\mu_y = 10/9, 10/7$. These curves were calculated using Eq. (B.6) when $\lambda_x = \lambda_y$, and from numerical integration of Eq. (B.5) when $\lambda_x \neq \lambda_y$.

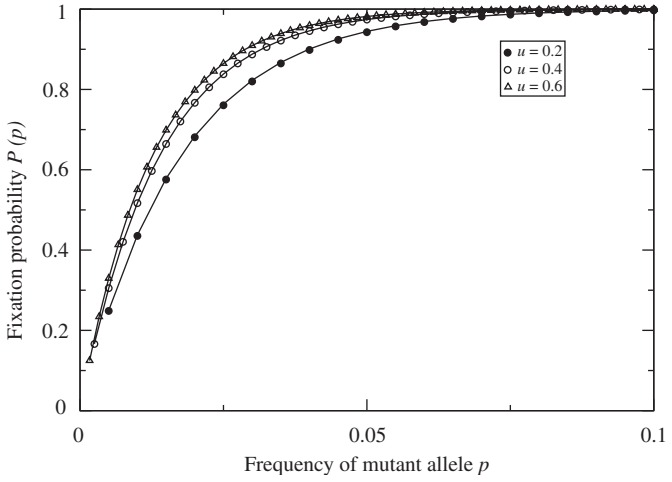

Fig. 6. Fixation probability of an advantageous type $\mathcal{Y}$ mutant $P(p)$ as a function of its initial frequency p. The solid lines give the asymptotic approximations (Eq. (17)), and the symbols the exact numerical calculations. The symbols always lie on the corresponding curve. This is shown for three different initial population densities, $u = 0.2, 0.4, 0.6$. The parameter values are $\lambda_y = 1.0, \mu_y = 0.5, \lambda_x = 1.0, \mu_x = 0.6$, and $K = 1000$. For these parameters $\bar{u}_1 = 0.4$.

the deterministic flow, increasing the probability that type $\mathcal{Y}$ fixes. Thus, the equivalent fixed population size system is larger than Ku. In contrast, if u is greater than $\bar{u}_1$, the initial decrease in population density is not accompanied by a rapid decrease in v. In a shrinking population, competitive differences are not so important. Starting with u greater than $\bar{u}_1$ increases the amount of time that a typical trajectory spends near the $v = 1$ axis, and increases the fixation probability of type $\mathcal{X}$. This corresponds to a decrease in the effective population size of the system.

This analysis depends on the effectiveness of our asymptotic approximation. In fact, Eq. (17) is remarkably good at estimating the fixation probability of an advantageous allele. This is illustrated by Fig. 6 where we compare the asymptotic prediction for the fixation probability with the exact numerical results for three different initial densities. The approximation holds provided u does not get very close to zero. The situation is quite different for fixation of deleterious mutants, where our approximations break down. This is discussed in the next section.

5.2. Fixation of deleterious mutants (type $\mathcal{X}$)

Near the $x = 0$ (or equivalently, $v = 0$) axis, there is a region of initial densities for which the asymptotic approximation is inaccurate for intermediate K values. In this region, we depend on numerics for our analysis. This region corresponds to the case of a deleterious mutant invading a resident population. The solid line in Fig. 7 shows the fixation probability for a single mutant of type $\mathcal{X}$, as a function of initial resident population number $N = uK$, calculated numerically. This shows that the

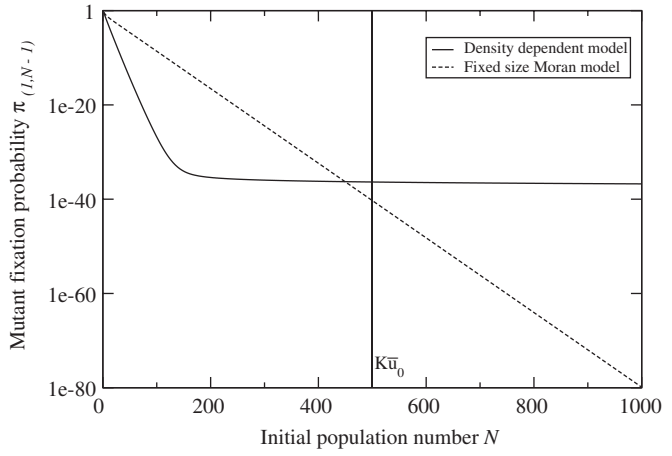

Fig. 7. Fixation probability, $\pi_{(1,N-1)}$, for a single deleterious mutant of type $\mathcal{X}$ invading a resident population of type $\mathcal{Y}$, as a function of the initial resident population number, N. The solid line gives the numerical calculation for the density-dependent model, and the dashed line gives the fixation probability for the equivalent fixed size Moran model, $(1 - 1/v)/(1 - (1/v)^N)$. The gray line indicates the resident demographic equilibrium, $N = \bar{u}_0 K \equiv (1 - \mu_y/\lambda_y)K$. The parameters used were $\lambda_x = 1, \lambda_y = 1, \mu_x = 0.6, \mu_y = 0.5$, and $K = 1000$. For these parameters $v = 5/6$. The y-axis is logarithmically scaled.

fixation probability decreases with N for all N. However, this decrease is initially rapid for small N, but then slows down. For a broad range of values of N near the demographic equilibrium of the resident type $\mathcal{Y}$, $\bar{u}_0 K = (1.0 - \mu_y/\lambda_y)K$, the fixation probability only decreases slowly with increasing N.

The qualitative explanation for this is that once N is large enough so that we are no longer in the corner region Section 4.3, then fixation probability is relatively insensitive

to N, since the deterministic dynamics will rapidly cause N to approach the resident equilibrium, $\bar{u}_0 K$, anyway.

This is quite different to the continuous, approximately exponential decrease in fixation probability with total population size that is predicted by the fixed size Moran model, the dashed line of Fig. 7. The deterministic change in population size for N significantly smaller than $\bar{u}_0 K$ decreases the fixation probability in the density-dependent model relative to the Moran model, and increases it for large initial N values. The two curves intersect at a population size somewhat smaller than $\bar{u}_0 K$.

For reasonably large initial resident population size, the fixation probability for a deleterious mutant will be close to that for the case $N = \bar{u}_0 K$. We will therefore focus on this case to investigate the effect of altering the mutant fitness on the fixation probability. Considering this case also removes the effect of initial changes in mean population size from the comparison with the fixed size model, so that any differences between the two will be due to demographic stochasticity alone. Assuming that the resident population of type $\mathcal{Y}$ is exactly at equilibrium, $N = \bar{u}_0 K = (1 - \mu_y/\lambda_y)K$, and that one individual then mutates, the relevant fixation probability will be $\pi_{(1,\bar{u}_0 K-1)}$. In Fig. 8 we give $\pi_{(1,\bar{u}_0 K-1)}$ as a function of $v = \lambda_x \mu_y / \lambda_y \mu_x$. The latter quantity gives the relative fitness of type $\mathcal{X}$ which can be altered either by changing its per capita death rate μ_x or the density-independent component of the birth rate λ_x. The solid line in Fig. 8 shows how the fixation probability depends on v in the first case, and the dashed line shows the dependence in the second case. This figure contains a slight abuse of our formalism in that type $\mathcal{X}$ is advantageous for some parameter values. The two cases are equivalent for advantageous and neutral mutations ($v \geqslant 1$). For deleterious mutations, the fixation probabilities are slightly—but consistently—higher when λ_x is reduced rather than μ_x increased. This indicates that $\pi_{(1,\bar{u}_0 K-1)}$can only approximately be described as a function of the single variable v.

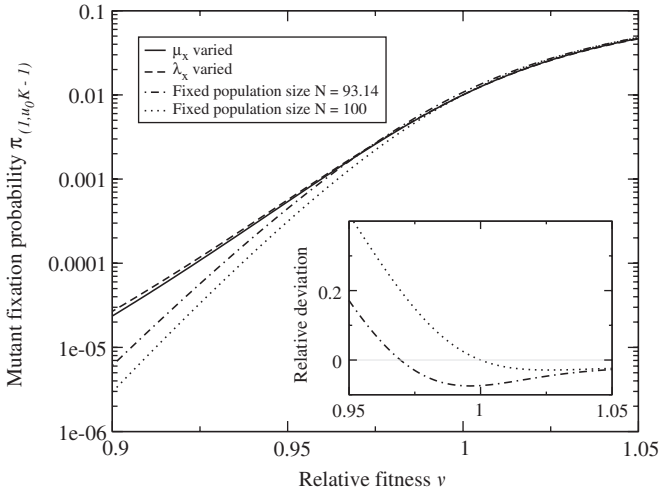

Fig. 8. Fixation probability, $\pi_{(1,\bar{u}_0 K-1)}$, for a single mutant of type $\mathcal{X}$ invading a resident population of type $\mathcal{Y}$, at the resident's demographic equilibrium $N = \bar{u}_0 K$. Fixation probability is shown as a function of relative fitness v, for μ_x varied whilst $\lambda_x = 1$ (solid line), and λ_x varied whilst $\mu_x = 0.75$ (dashed line). The other parameters were $\lambda_y = 1, \mu_y = 0.75$, and $K = 400$. The dotted and dash-dotted lines give the fixation probability for fixed size Moran models, $\pi^\dagger = (1 - 1/v)/(1 - (1/v)^N)$, with population size N equal to the resident demographic equilibrium, $\bar{u}_0 K = 100$, and the harmonic mean of the quasi-stationary distribution, 93.14, respectively. The y-axis is logarithmically scaled. The inset graph shows the relative deviation of the density-dependent model for μ_x varied, $(\pi - \pi^\dagger)/\pi$, from the two fixed size systems near neutrality.

In order to determine the effect of demographic stochasticity on fixation, we also show in Fig. 8 the fixation probability as a function of v for the equivalent system of fixed population size. This is simply Eq. (2) with N fixed at the resident equilibrium population size, $\bar{u}_0 K$. The results are striking; for deleterious mutants the fixation probability is increased by a fluctuating population size, whereas the fixation probabilities are practically equivalent for advantageous alleles. The effect gets larger as the relative fitness v is reduced, and is of significant size (note the log scale), so that the fixation probability is an order of magnitude larger for the fluctuating population when $v = 0.9$.

It has been shown in previous work that the effective population size for a fluctuating population should be equal to the harmonic mean of the population size (Ewens, 1967; Otto and Whitlock, 1997). We test this in Fig. 8, where we show the fixation probability for a Moran model with population size fixed to the harmonic mean of the resident population size, $N = 93.14$. This results in an over-estimation of fixation probability for neutral and weakly deleterious mutations and an under-estimation for strongly deleterious mutations. This is clearly illustrated by the inset of Fig. 8 which shows the deviance of the fixed population size approximations from the density-dependent case. Using a harmonic mean fixed population size does give a good approximation for a range of mutation strengths, near where the deviance intersects the zero axis in the inset, but this is a narrow range. The inset also shows that for neutral and weakly advantageous mutations, the Moran model with population size equal to the initial population size, $\bar{u}_0 K$, is a better approximation than using a harmonic mean population size, while for strongly advantageous mutations, both fixed size approximations do well: the deviance converges on a small negative value.

The qualitative explanation for this phenomenon seems to be that for an advantageous mutant, fixation depends only on the invading population reaching some critical size. Once this occurs, the increased growth rate of the mutant population—the deterministic flow—ensures that fixation will happen. Consider a small population of a mutant invading a resident population: its per capita growth rate will be approximately $\lambda_x(1 - \bar{u}_0) = \lambda_x \mu_y / \lambda_y$ and its per capita death rate will be μ_x. It is a standard result from birth-and-death processes that a population with births occurring at a per capita rate b and deaths at per capita rate d, $b > d$, will go extinct with probability d/b, and grow

indefinitely otherwise (van Kampen, 1992). In our case, this gives a fixation probability of $1 - 1/v$, which for large N is equivalent to the prediction from the Moran model irrespective of the value of N. The close correspondence of this approximation to the numerical calculations suggests that fixation is determined by the deterministic dynamics when the number of mutants is no longer small.

In contrast, for a deleterious mutant, even when its population has reached a considerable size, its fixation is not ensured. This is because its fixation must occur against the deterministic flow. Consequently, a fluctuating resident population size significantly increases the fixation probability of a deleterious mutation, as compared to that in a population of fixed size. This likely occurs because, in some instances, invasion will coincide with a negative fluctuation in the resident population, decreasing the distance against the deterministic flow that the mutant must prevail for fixation to occur.

We investigate this phenomenon further in Fig. 9, where the upper surface shows the fixation probability of a deleterious mutant invading a resident population, as a function of the mean and the standard deviation of the resident population size prior to invasion. The mean population size, $\bar{N} = \langle N \rangle$, and the standard deviation, $\sigma = \langle (N - \bar{N})^2 \rangle^{0.5}$, are both calculated by averaging over the quasi-stationary distribution of the resident. As discussed at the start of this section $\bar{N} \simeq (1 - \mu_y/\lambda_y)K$ and $\sigma \simeq \sqrt{\mu_y K/\lambda_y}$. Consequently, increasing μ_y whilst increasing K (so as to keep $\bar{N}$ fixed) increases σ. The fixation probability is calculated as an average over the quasi-stationary distribution $\bar{\pi} = \langle \pi_{(1,N-1)} \rangle$.

The lowest surface in Fig. 9 gives the Moran model fixation probability when the mean population size $\bar{N}$ is used. Note that this is independent of σ. The surface above that shows the result when the harmonic mean population size is used in the Moran model. This fixation probability does increase with increasing fluctuation size as the harmonic mean gets smaller. However, for all fluctuation sizes the fixation probabilities are below those of the density-dependent case (upper surface). In all three cases the fixation probability decreases exponentially with resident population size. As the fluctuations become larger, the difference between the density-dependent and fixed size models increases. This confirms our hypothesis that demographic stochasticity in the resident population increases the fixation probability of deleterious mutants.

In this figure, only a relatively small range of mean population sizes $\bar{N}$ are shown. This is done so that the important points, the effect of σ on the fixation probability in the density-dependent model and that the three surfaces coincide as σ tends to zero for all $\bar{N}$, are clear. The same patterns will persist over all $\bar{N}$ values, provided $\bar{N}$ is large enough relative to the fluctuation sizes that a long-lived resident quasi-stationary distribution is formed. The surfaces in Fig. 9 are only shown for one value of the fitness ratio v. The effect of decreasing v is to increase the difference between the fixed population and fluctuating population size models, as is shown in Fig. 8.

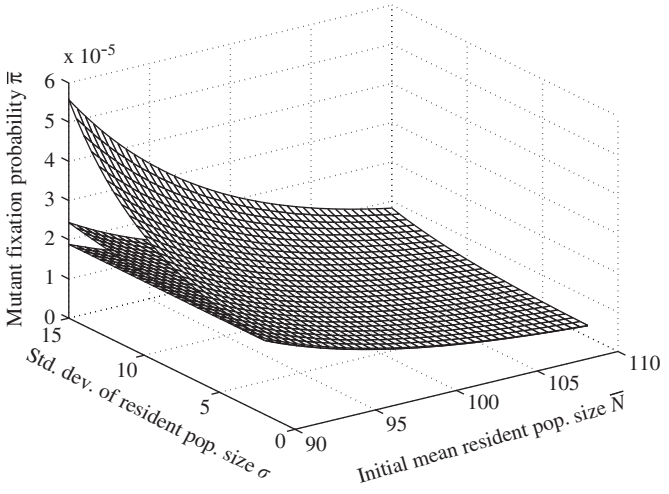

Fig. 9. The upper surface gives the fixation probability of a deleterious mutant of type $\mathcal{X}$ invading a resident population of type $\mathcal{Y}$, as a function of the mean, $\bar{N}$, and the standard deviation, σ, of the resident population size prior to invasion. Birth rates were kept fixed $\lambda_x = \lambda_y = 1$ for both types. For each mean population size, the resident death rate μ_y was increased from zero, with K increased from $\bar{N}$, so as to keep $\bar{N}$ approximately fixed. The deleterious mutant has a death rate that was a fixed multiple of the resident, such that $v = \mu_y/\mu_x = 10/11$. The lowest surface shows fixation probabilities for a Moran model with population number equal to the mean of the population size, $\bar{N}$. The surface above that gives the Moran model result when the harmonic mean population size is used.

6. Mean mutant fixation times

In this final section of results, we extend our analysis of fixation and density-dependent population dynamics by investigating the mean time to fixation for a mutant individual, conditional on fixation of that mutant occurring. The results for a single mutant of type $\mathcal{X}$ invading a resident population of type $\mathcal{Y}$ near the resident's demographic equilibrium are shown as a solid line in Fig. 10. The mean fixation times are given as a function of the relative fitness of type $\mathcal{X}$, v. In a second abuse of our formalism, the type $\mathcal{X}$ mutant can be advantageous as well as deleterious.

In Fig. 10, we also show the mean fixation times for fixed size models with N equal to the initial population size, which are taken to be the resident demographic equilibrium $\bar{u}_0 K$, and the integer value nearest to the harmonic mean of the population size. Comparing the lines we see that all three have a characteristic humped shape (Ewens, 1979). It is perhaps not surprising that average fixation time should decrease as mutants become more advantageous. It is less obvious that they should decrease as mutants become more deleterious. The key is that the fixation times are conditional on fixation having occurred. The more deleterious a mutation, the fewer steps backward it can accommodate and still fix. The average number of steps and therefore time decreases.

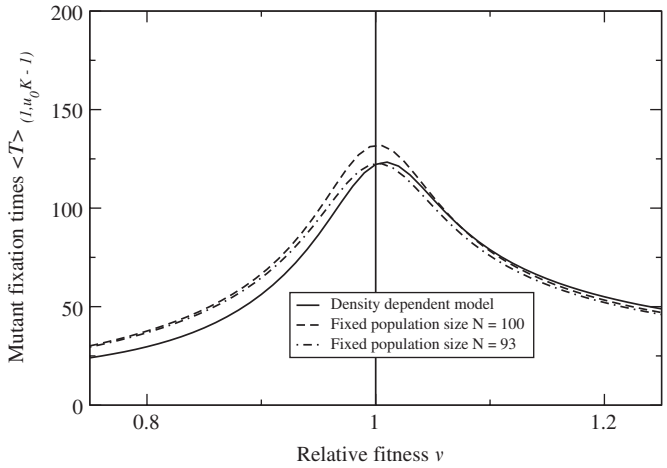

Fig. 10. Mean fixation time, $\langle T\rangle_{(1,\bar{u}_0K-1)}$, for a single mutant of type $\mathcal{X}$ invading a resident population of type $\mathcal{Y}$, at the resident's demographic equilibrium $N = \bar{u}_0K \equiv (1-\mu_y/\lambda_y)K$. Mean fixation time is shown as a function of relative fitness at $v = \lambda_x\mu_y/\lambda_y\mu_x$. The relative fitness was varied by altering the mutant death rate μ_x. The other parameters were $\lambda_x = \lambda_y = 1, \mu_y = 0.75$ and $K = 400$. The solid line gives results for the density-dependent model, and the dashed and dot-dashed lines fixed size Moran models, with N equal to the resident demographic equilibrium $\bar{u}_0K = 100$ and the nearest integer value to the harmonic mean of the population size $N = 93$, respectively. The gray vertical line shows the line $v = 1$.

Comparing the density-dependent model (solid line) with the fixed size model with N set at the initial population size (dashed line), we see that for deleterious and neutral mutations fixation times are reduced in the density-dependent model. This supports our hypothesis that demographic stochasticity increases the fixation probability for deleterious mutations through fluctuations that reduce the resident population size. If in order to fix, deleterious mutants only need to reach a total number that is smaller than the resident's demographic equilibrium, then this will occur in a shorter average time. This effect also appears to operate for neutral mutations, but not for advantageous mutants, where the fixation times are very similar for fixed and fluctuating population sizes.

The reduction in fixation time for neutral mutations is correctly accounted for by using the harmonic mean of the population size rather than the initial population size in the fixed size model. However, for deleterious mutations, the harmonic mean still over-estimates the fixation time. This is what we might expect, given that the harmonic mean should only be a good approximation to the effective population size if the time-scale of fixation is long compared to the time-scale of fluctuations in the population size (Ewens, 1967, 1979).

7. Discussion

In this paper we studied fixation probabilities in a model with two alleles where the birth rates of each allele depends on the total population density. This allowed us to investigate the effects on fixation of both deterministic changes in population number, for populations starting away from demographic equilibrium, and of fluctuations in population size, for populations close to equilibrium. We considered both advantageous and deleterious mutants, and found that in the first case, deterministic changes had the greater effect on the fixation probabilities, while in the second case, fluctuations were key. We examined mutant fixation times, which reinforced this point. We also derived the fixation probabilities for populations of small total population density.

7.1. Fixation of advantageous mutants

We derived an asymptotic approximation for the fixation probability of an advantageous allele, as a function of the initial mutant frequency and the total population number. We showed that this approximation was accurate at intermediate system sizes, provided that the initial frequencies were not very large and the initial total population densities were not very small. This is, to the best of our knowledge, the first time that such an expression has been derived for a model where the birth-and-death processes responsible for allele fixation also determine the changes in total population numbers. Expressions have been derived previously for fixation in populations of changing size, e.g., Kimura and Ohta (1974), Otto and Whitlock (1997), but for these models the population size was effectively an externally imposed constraint.

We found that the fixation probability for an advantageous mutant invading a population close to the demographic equilibrium of the resident was equal to Kimura's diffusion approximation applied to a haploid population with a variance effective size that was half the census size (Kimura, 1957, 1962). This result for the variance effective size is what we would expect for a fixed population size Moran model (Ewens, 1979). This implies that the fluctuations in resident population number in our model have little effect on the fixation probability. This is surprising, given that other models of allele fixation in fluctuating populations predict that the effective population size should be reduced to the harmonic mean of the population number (Ewens, 1967; Otto and Whitlock, 1997).

Our asymptotic approximation could also be applied to fixation in populations with initial density not equal to the resident demographic equilibrium. We were able to show for any parameter values, that the effective population size was increased in growing populations and decreased in shrinking populations. In the case of equal birth rates, we were able to explicitly derive an expression for the effective population size, finding that it was the reciprocal of a linear function of the initial population density. In other cases, determination of the effective population size requires the numerical solution of an integral. Our result for the effect of changes in population size on the fixation of advantageous alleles agrees with previous findings (Kimura and

Ohta, 1974; Otto and Whitlock, 1997). However, as argued above, our framework is more natural, and our approximations, which are remarkably good at intermediate system sizes, will become exact in the limit of infinitely large systems. Our expressions are also not limited to mutants that are similar to the resident, or populations that are growing slowly. They hold over all parameter values.

In addition, our framework, by explicitly modelling the density-dependent interactions, provides some unique insights into fixation of advantageous alleles in populations of changing size. In our model, an advantageous mutant can have either a higher birth rate or a lower death rate, or indeed both, although for simplicity we do not present the latter case. If we compare $\Psi(u)$ for mutants that have a higher birth rate with those that have a lower death rate, but the same fitness advantage relative to the resident, v—compare the dotted with the solid lines and dot-dashed with the dashed lines of Fig. 5—we find that mutants with the higher birth rates are more likely to fix in growing populations and less likely to fix in shrinking populations. This occurs because an increased birth rate allows a mutant to exploit the reduced density dependence in a small growing population. Conversely, in a shrinking population, a reduced death rate that increases a mutant probability of surviving to a time where total population sizes is smaller, is more useful than an increased birth rate. This also illustrates that when demographics are incorporated into allele fixation, then fixation probabilities are not a simple function of relative fitness v, in contrast to a recent claim (Sella and Hirsh, 2005).

A recent study by Lambert considered fixation in a model very similar to ours but with density-dependent death rates rather than birth rates (Lambert, 2006). However, the approximations he derived for the fixation probability were made under the assumption of invasion by a mutant infinitesimally similar to the resident. He represented the fixation probability by a series solution in powers of the selective difference and truncated this series to second order, leading to a solution that was quadratic in the initial mutant frequency. Such an approach does provide some insight into what determines the fitness of allele, but the actual solutions are not guaranteed to be close to the real solution, except in the limit of neutrality. Moreover, he did not compare his approximation with numerical results. The fact that our asymptotic solution, which is exact in the limit of large system sizes, was of an exponential form suggests that the range of applicability of Lambert's approximation is very small.

7.2. Fixation of deleterious mutants

Provided the population density is reasonably large, the fixation probability for deleterious mutants is relatively insensitive to initial population density, unlike the case of advantageous mutants. However, as we demonstrated numerically, the fixation probability is influenced by the demographic stochasticity of the resident population. The larger the size of the fluctuations in the resident population number, the greater the probability of fixation of deleterious alleles.

We showed that the behavior of the model in this case cannot simply be described by that of a Moran model with an effective population size equal to the harmonic mean of the resident population size. This is in contrast to previous theoretical findings (Ewens, 1967; Otto and Whitlock, 1997). The harmonic mean is smaller than the resident demographic equilibrium population size, and hence using the harmonic mean increases the fixation probability of deleterious alleles, but this increase is not as large as we observe in our model. Further, the size of the increase in the fixation probability relative to the fixed size model increases from zero at neutrality as the mutant becomes increasingly disadvantageous. This suggests that the Moran effective population size must be a function of the mutant parameters. We tested this by fitting an effective population size to the data in Fig. 8. We were unable to determine a single effective population size that could fit the fixation probabilities from the density-dependent model.

This phenomenon has consequences for the accelerating accumulation of deleterious alleles in haploid populations, the so-called 'mutational meltdown' (Lynch et al., 1993; Lande, 1994). The mutational meltdown is a positive feedback effect; small population sizes lead to fixation of deleterious alleles, which then cause a reduction in population size, thereby increasing the probability of fixation of deleterious mutations. Eventually, when the birth rate is reduced to zero, the population becomes extinct.

Our result shows that if demographic stochasticity is incorporated into models of allele fixation, then firstly, the fixation probabilities of deleterious mutations will be increased, and secondly, a further positive feedback effect will exist. A reduced birth rate or increased death rate, will increase the size of the fluctuations in population size, increasing the probability of further fixations. Demographic stochasticity will thus reduce the time to mutational meltdown. This effect is ignored in the standard models which assume a population size that is fixed until the deleterious mutant is fixed (Lynch et al., 1993; Lande, 1994).

7.3. Fixation times

We numerically investigated mean fixation times for both deleterious and advantageous mutants invading a population near its demographic equilibrium. The results showed that mean fixation times for deleterious mutants are reduced by demographic stochasticity. This too would contribute to reducing the time for mutational meltdown in haploid populations. Interestingly this effect occurred for neutral mutations too. Since the mean time for a sample consisting of the whole population to coalesce—derive from a single common ancestor—going backwards in time,

is equal to the mean fixation time, then this is related to the observation that fluctuations should reduce coalescence times (Kingman, 1982). In fact, for neutral mutations, an effective fixed population size equal to the harmonic mean of the resident population size correctly predicts the fixation time (Jagers and Sagitov, 2004).

7.4. Behavior near the origin

We saw that for small populations, the first-order approximation to the fixation probability (13) is the probability that type Y becomes extinct at some time at which the number of individuals of type X is nonzero, for independent, density-independent birth–death processes. This is as we would expect: at small sizes, density-dependent effects are negligible, while to fix, either type must escape to large sizes where the probability of extinction due to demographic effects is small. Thus, for small populations, our model simplifies to be very similar to early models of Fisher and Haldane (e.g. Fisher, 1922; Haldane, 1927), that use branching processes to model population growth and fixation.

7.5. Further applications and extensions of the model

As mentioned in the text, in this paper we only consider fixation when the two types have different equilibrium population densities. The other case, when the types have the same ratio of birth to death rates and hence equilibrium population densities, has a different deterministic dynamics and therefore requires different mathematical techniques. (Parsons and Quince, submitted).

The model as formulated here has a number of other applications. In general, it provides a better framework for considering the interaction of demographics and allele fixation than previously defined models. We intend to apply it to mutational meltdown and quantify the statements made in Section 7.2. It could be used to describe competing parasite strains exploiting the same host population in a SIS model or competing bacterial strains on a substrate of fixed size. Interesting extensions of the model would include looking at the case of general density dependence or developing the equivalent diploid model. In summary we think this study is a significant step towards a rigorous integration of population genetics and population dynamics.

Acknowledgments

This work was supported by a Discovery grant and a Strategic Project grant from the Natural Sciences and Engineering Research Council of Canada to Peter Abrams. We wish to thank Claus Rueffler, Peter Abrams, Lee Worden and two anonymous reviewers for helpful comments on earlier versions of this manuscript.

Appendix A. Subboundary layer solution near $(\bar{u}_1, 1)$

To find the subboundary layer solution near $(\bar{u}_1, 1)$, which we will denote $\hat{\pi}$, we introduce stretched coordinates ξ and η. Let

$$u = \bar{u}_1 - \xi K^{\alpha} \quad \text{and} \quad v = 1 - \eta K^{\beta}.$$

By choosing α and β so that the highest order derivatives are preserved when we take the limit as $K \to \infty$, we stretch the region in which the deterministic flow and diffusion are of equal magnitude to the whole of the $\xi\eta$-plane. Substituting into (5), we find that $\alpha = -\frac{1}{2}$ and $\beta = -1$. Thus, $\hat{\pi}$, satisfies

$$-(\lambda_x - \mu_x)\xi \frac{\partial \hat{\pi}}{\partial \xi} - \left(\frac{\lambda_x\mu_y - \lambda_y\mu_x}{\lambda_x}\right)\eta \frac{\partial \hat{\pi}}{\partial \eta} + \frac{\mu_x(\lambda_x - \mu_x)}{\lambda_x}\frac{\partial^2 \hat{\pi}}{\partial \xi^2} + \frac{\lambda_x\mu_y + \lambda_y\mu_x}{2(\lambda_x - \mu_x)}\eta \frac{\partial^2 \hat{\pi}}{\partial \eta^2} = 0.$$

$$\hat{\pi}(\xi, 0) = 1,$$

$$\lim_{\eta \to \infty} \hat{\pi}(\xi, \eta) = 0. \tag{A.1}$$

The second boundary condition arises from the need to have $\hat{\pi}$ match the outer solution π_0 in the interior of Ω.

We next find a separable solution to this equation. Solving and imposing the boundary conditions, we find

$$\hat{\pi}(\xi, \eta) = e^{-2\bar{u}_1((1-v)/(1+v))\eta}, \tag{A.2}$$

where $v = \lambda_x\mu_y/\lambda_y\mu_x$ is the relative fitness of the invading type.

Appendix B. Complete boundary layer solution near $\partial\Omega_1$

We now look for a solution on the remainder of the boundary layer. We let $v = 1 - \eta K^{-1}$, but leave u unchanged. Substituting into (5) and letting $K \to \infty$, we find that $\tilde{\pi}(u, \eta)$ satisfies

$$[\lambda_x u(1-u) - \mu_x u]\frac{\partial \tilde{\pi}}{\partial u} - \eta[(\lambda_x - \lambda_y)(1-u) - (\mu_x - \mu_y)]\frac{\partial \tilde{\pi}}{\partial \eta} + \frac{1}{2}\frac{\eta}{u}[\lambda_y(1-u) + \mu_y]\frac{\partial^2 \tilde{\pi}}{\partial \eta^2} = 0,$$

$$\tilde{\pi}(u, 1) = 1,$$

$$\lim_{\eta \to \infty} \tilde{\pi}(u, \eta) = 0. \tag{B.1}$$

We seek a solution to (B.1) consistent with $\hat{\pi}$, so we look for a similarity solution of the form

$$\tilde{\pi}(u, \eta) = e^{-\eta/\Phi(u)} \tag{B.2}$$

such that

$$\lim_{u \to \bar{u}_1} \Phi(u) = \frac{1+v}{2\bar{u}_1(1-v)}. \tag{B.3}$$

This is equivalent to making a change of coordinates $\eta = \zeta\Phi(u)$ such that (B.1) becomes separable, and solving the resulting equation for $\tilde{\pi}$.

Substituting (B.2) into (B.1) and simplifying yields a linear ordinary differential equation for Φ:

$$[\lambda_x u(1-u) - \mu_x u]\Phi' + [(\lambda_x - \lambda_y)(1-u) - (\mu_x - \mu_y)]\Phi + \frac{1}{2u}[\lambda_y(1-u) + \mu_y] = 0. \tag{B.4}$$

After imposing the consistency condition (B.3), this has solution

$$\Phi(u) = \int_u^{\bar{u}_1} \left(\frac{z}{u}\right)^{1-(\lambda_y-\mu_y)/(\lambda_x-\mu_x)} \times \left(\frac{\lambda_x(1-z)-\mu_x}{\lambda_x(1-u)-\mu_x}\right)^{(\lambda_y\mu_x-\lambda_x\mu_y)/\lambda_x(\lambda_x-\mu_x)} \times \frac{\lambda_y(1-z)+\mu_y}{2z[\lambda_x z(1-z)-\mu_x z]}\, dz. \tag{B.5}$$

A calculation using l'Hôpital's rule shows that Φ has the correct limit as $u \to \bar{u}_1$. From the expression for Φ, we can see that it is strictly positive, while computing its derivative, we see that Φ is strictly increasing.

In the special case where $\lambda_x = \lambda_y = \lambda$, looking for a regular series solution for $\Phi(u)$ yields a simple closed form for $\Phi(u)$:

$$\Phi(u) = \frac{\lambda+\mu_y}{2(\lambda-\mu_y)}\frac{1}{u} + \frac{\lambda\mu_y}{(\lambda-\mu_y)(\mu_x-\mu_y)}. \tag{B.6}$$

Appendix C. Corner layer solution near the origin

We will use coordinates x and y to describe the behavior near the origin.

Near the origin, we need to introduce a correction to take into account the increased probability of extinction at small population sizes. We do this by introducing a corner layer at (0,0), with coordinates ξ and η given by $x = \xi K^{-1}$ and $y = \eta K^{-1}$. Substituting these into (4) and taking the limit as $K \to \infty$, we find that the corner layer solution $\check{\pi}(\xi,\eta)$ satisfies:

$$(\lambda_x-\mu_x)\xi\frac{\partial\check{\pi}}{\partial\xi} + (\lambda_y-\mu_y)\eta\frac{\partial\check{\pi}}{\partial\eta} + \frac{1}{2}\left\{(\lambda_x+\mu_x)\xi\frac{\partial^2\check{\pi}}{\partial\xi^2} + (\lambda_y+\mu_y)\eta\frac{\partial^2\check{\pi}}{\partial\eta^2}\right\} = 0 \tag{C.1}$$

with the boundary conditions

$$\check{\pi}(\xi,0) = 1 \quad \text{if } \xi > 0,$$
$$\check{\pi}(0,\eta) = 0 \quad \text{if } \eta > 0.$$

The probability $p(\xi,\eta,\xi_0,\eta_0,t)$ that there are ξ individuals of type X and η individuals of type Y at time t, given initial densities ξ_0 and η_0, satisfies the corresponding forward Fokker–Planck equation

$$\begin{aligned}\frac{\partial p}{\partial t} &= -\left\{\frac{\partial}{\partial\xi}\left[(\lambda_x-\mu_x)\xi p(\xi,\eta,\xi_0,\eta_0,t)\right] + \frac{\partial}{\partial\eta}\left[(\lambda_y-\mu_y)\eta p(\xi,\eta,\xi_0,\eta_0,t)\right]\right\} \\ &\quad + \frac{1}{2}\left\{\frac{\partial^2}{\partial\xi^2}\left[(\lambda_x+\mu_x)\xi p(\xi,\eta,\xi_0,\eta_0,t)\right] + \frac{\partial^2}{\partial\eta^2}\left[(\lambda_y+\mu_y)\eta p(\xi,\eta,\xi_0,\eta_0,t)\right]\right\} \\ &= -\nabla\bullet J(\xi,\eta,\xi_0,\eta_0,p), \\ &\quad p(\xi,\eta,\xi_0,\eta_0,0) = \delta((\xi,\eta)-(\xi_0,\eta_0)).\end{aligned}$$

Thus, near the origin, we may neglect density dependence, and the numbers of individuals of type X and the number of individuals of type Y satisfy two independent Feller processes (Feller, 1951): we may write $p(\xi,\eta,\xi_0,\eta_0,t) = p_1(\xi,\xi_0,t)p_2(\eta,\eta_0,t)$, where

$$\frac{\partial p_1}{\partial t} = -\frac{\partial}{\partial\xi}\left[(\lambda_x-\mu_x)\xi p_1(\xi,t)\right] + \frac{1}{2}\frac{\partial^2}{\partial\xi^2}\left[(\lambda_x+\mu_x)\xi p_1(\xi,t)\right],$$

$$\frac{\partial p_2}{\partial t} = -\frac{\partial}{\partial\eta}\left[(\lambda_y-\mu_y)\eta p_2(\eta,t)\right] + \frac{1}{2}\frac{\partial^2}{\partial\eta^2}\left[(\lambda_y+\mu_y)\eta p_2(\eta,t)\right], \tag{C.2}$$

$$p_1(\xi,\xi_0,0) = \delta(\xi-\xi_0),$$
$$p_1(\eta,\eta_0,0) = \delta(\eta-\eta_0).$$

In Feller (1951), exact solutions are given for (C.2), which may be used to construct a solution to (C.1) (Matkowsky et al., 1983; Gardiner, 2004). Let $\mathbf{n}$ be the outward unit normal to $\partial\Omega_1$. Then,

$$\begin{aligned}\check{\pi}(\xi,\eta) &= \int_0^\infty\int_0^\infty J(\xi',\xi,0,\eta,p)\bullet\mathbf{n}\, d\xi'\, dt \\ &= \int_0^\infty\int_0^\infty \left((\lambda_y-\mu_y)\eta' p(\xi',\eta',\xi,\eta,t) - \frac{1}{2}\frac{\partial^2}{\partial\eta^2}\left[(\lambda_y+\mu_y)\eta p(\xi',\eta',\xi,\eta,t)\right]\right)\Big|_{\eta'=0} d\xi'\, dt \\ &= \int_0^\infty\int_0^\infty p_1(\xi',\xi,t)\, d\xi' \left((\lambda_y-\mu_y)\eta' p_2(\eta',\eta,t) - \frac{1}{2}\frac{\partial^2}{\partial\eta^2}\left[(\lambda_y+\mu_y)\eta p_2(\eta',\eta,t)\right]\right)\Big|_{\eta'=0} dt \\ &= \int_0^\infty \left(1 - e^{-\frac{\lambda_x-\mu_x}{\lambda_x+\mu_x}\xi\frac{1}{1-e^{-(\lambda_x-\mu_x)t}}}\right) f(t)\, dt,\end{aligned}$$

where

$$f(t) = -\frac{(\lambda_y-\mu_y)^2\eta e^{-(\lambda_y-\mu_y)t}}{(\lambda_y+\mu_y)\left(1-e^{-(\lambda_y-\mu_y)t}\right)^2} e^{-\frac{\lambda_y-\mu_y}{\lambda_y+\mu_y}\eta\frac{1}{1-e^{-(\lambda_y-\mu_y)t}}}$$

is the flux of η' at 0 (Feller, 1951, the probability that type Y becomes extinct at time t. $\breve{\pi}_0$ is then the integral over all time of the probability that type Y becomes extinct at some time t when the number of individuals of type X is nonzero. Making a change of variable $w = 1-e^{-(\lambda_y-\mu_y)t}$, we may write $\breve{\pi}$ more compactly as

$$2\int_0^1 \left(1-e^{-2\frac{\lambda_x-\mu_x}{\lambda_x+\mu_x}\frac{\xi}{1-(1-w)^{\frac{\lambda_x-\mu_x}{\lambda_y-\mu_y}}}}\right)\frac{\lambda_y-\mu_y}{\lambda_y+\mu_y}\frac{\eta}{w^2}e^{-2\frac{\lambda_y-\mu_y\eta}{\lambda_y+\mu_y w}}dw$$

Appendix D. Matched asymptotic solution

We complete our asymptotic analysis by using Van Dyke's matching rule, e.g., Hinch (1991) to combine the near-origin asymptotic solution with the interior and boundary layer solutions to obtain a single asymptotic expression valid everywhere in Ω.

Near the origin, we can write $\tilde{\pi}$ in terms of coordinates ξ and η:

$$\tilde{\pi} = e^{-\frac{\eta}{\left(\frac{\xi+\eta}{K}\right)\Phi\left(\frac{\xi+\eta}{K}\right)}}. \tag{D.1}$$

Since Φ has residue $-\frac{\lambda_y+\mu_y}{2(\lambda_y-\mu_y)}$ at $u=0$, we see that

$$\lim_{K\to\infty}\tilde{\pi}(\xi,\eta) = e^{2\left(\frac{\mu_y-\lambda_y}{\mu_y+\lambda_y}\right)\eta}.$$

Now, near Ω_1 but away from the origin, we can write

$$\breve{\pi} = 2\int_0^1 \left(1-e^{-2\frac{\lambda_x-\mu_x}{\lambda_x+\mu_x}\frac{Kx}{1-(1-w)^{\frac{\lambda_x-\mu_x}{\lambda_y-\mu_y}}}}\right)\frac{\lambda_y-\mu_y}{\lambda_y+\mu_y}\frac{\eta}{w^2}e^{-2\frac{\lambda_y-\mu_y\eta}{\lambda_y+\mu_y w}}dw$$

so

$$\begin{aligned}\lim_{K\to\infty}\breve{\pi}(x,\eta) &= 2\int_0^1 \frac{\lambda_y-\mu_y}{\lambda_y+\mu_y}\frac{\eta}{w^2}e^{-2\frac{\lambda_y-\mu_y\eta}{\lambda_y+\mu_y w}}dw\\ &= e^{2\left(\frac{\mu_y-\lambda_y}{\mu_y+\lambda_y}\right)\eta}.\end{aligned}$$

In particular, as K becomes large, the two solutions have a common limit on an intermediate scale. Adding the two solutions and subtracting this common limit yields a uniform approximation to π:

$$\pi(x,y) = e^{-\frac{Ky}{(x+y)\Phi(x+y)}} - 2\int_0^1 \frac{\lambda_y-\mu_y}{\lambda_y+\mu_y}\frac{Ky}{w^2}e^{-2\frac{\lambda_x-\mu_x}{\lambda_x+\mu_x}\frac{Kx}{1-(1-w)^{\frac{\lambda_x-\mu_x}{\lambda_y-\mu_y}}}-2\frac{\lambda_y-\mu_y}{\lambda_y+\mu_y}\frac{Ky}{u}}dw.$$

References

Crow, J.F., Morton, N.E., 1955. Measurement of gene frequencey drift in small populations. Evolution 9, 202–214.

Davis, T.A., 2004. Algorithm 832: UMFPACK, an unsymmetric-pattern multifrontal method. ACM Trans. Math. Software 30, 196–199.

Ewens, W.J., 1967. The probability of survival of a new mutant in a fluctuating environment. Heredity 22, 438–443.

Ewens, W.J., 1979. Mathematical Population Genetics. Springer, Berlin.

Feller, W., 1951. Two singular diffusion problems. Ann. of Math. 54 (1), 173–182.

Felsenstein, J., 1971. Inbreeding and variance effective numbers in populations with overlapping generations. Genetics 68, 581–597.

Fisher, R.A., 1922. On the dominance ratio. Proc. Roy. Soc. Edinburgh 42, 321–341.

Fisher, R.A., 1958. The Genetical Theory of Natural Selection, second ed. Dover, New York.

Gardiner, C.W., 2004. Handbook of Stochastic Methods for Physics, Chemistry and the Natural Sciences. Springer, Berlin, Heidelberg.

Grasman, J., van Herwaarden, O.A., 1999. Asymptotic Methods for the Fokker–Planck Equation and the Exit Problem in Applications. Springer, Berlin, Heidelberg.

Gurney, W.S.C., Nisbet, R.M., 1978. Single species population fluctuations in patchy environments. Am. Nat. 112, 1075–1090.

Haldane, J.B.S., 1927. A mathematical theory of natural and artificial selection. Part V: selection and mutation. Proc. Cambridge Philos. Soc. 23, 838–844.

Hinch, E.J., 1991. Perturbation Methods. Cambridge University Press, Cambridge.

Jacquez, J.A., Simon, C.P., 1993. The stochastic SI model with recruitment and deaths. I. Comparison with the closed SIS model. Math. Biosci. 117, 77–125.

Jagers, P., Sagitov, S., 2004. Convergence to the coalescent in populations of substantially varying size. J. Appl. Probab. 41, 368–378.

Kevorkian, J., Cole, J.D., 1996. Multiple Scale and Singular Perturbation Methods. Springer, New York Inc, New York.

Kimura, M., 1957. Some problems of stochastic processes in genetics. Ann. Math. Stat. 28, 882–901.

Kimura, M., 1962. On the probability of fixation of mutant genes in a population. Genetics 47, 713–719.

Kimura, M., Ohta, T., 1974. Probability of gene fixation in an expanding finite population. Proc. Natl. Acad. Sci. 71, 3377–3379.

Kingman, J.F.C., 1982. On the genealogy of large populations. J. Appl. Probab. 19A, 27–43.

Lambert, A., 2006. Probability of fixation under weak selection: a branching process unifying approach. Theor. Popul. Biol. 69, 419–441.

Lande, R., 1994. Risk of population extinction from fixation of new deleterious mutations. Evolution 48, 1460–1469.

Lynch, M., Bürger, R., Butcher, D., Gabriel, W., 1993. The mutational meltdown in asexual populations. J. Heredity 84, 339–344.

Matkowsky, B.J., Schuss, Z., Tier, C., 1983. Diffusion across characteristic boundaries with critical points. SIAM J. Appl. Math. 43, 673–695.

Moran, P.A.P., 1958. Random processes in genetics. Proc. Cambridge Philos. Soc. 54, 60–71.

Nåsell, I., 2001. Extinction and quasi-stationarity in the Verhulst logistic model. J. Theor. Biol. 211, 11–27.

Newman, T.J., Ferdy, J.-B., Quince, C., 2004. Extinction times and moment closure in the stochastic logistic process. Theor. Popul. Biol. 65, 115–126.

Nisbet, R.M., Gurney, W.S., 1982. Modelling Fluctuating Populations. Wiley, New York.

Otto, S.P., Whitlock, M.C., 1997. The probability of fixation in populations of changing size. Genetics 146, 723–733.

Parsons, T.L., Quince, C., submitted. Fixation in haploid populations exhibiting density dependence II: the quasi-neutral case. Theor. Popul. Biol.

Roozen, H., 1989. An asymptotic solution to a two-dimensional exit problem arising in population dynamics. SIAM J. Appl. Math. 49, 1810–1973.

Sella, G., Hirsh, A.E., 2005. The application of statistical physics to evolutionary biology. Proc. Natl. Acad. Sci. 102, 9541–9546.

Stewart, W.J., 1994. Introduction to the Numerical Solution of Markov Chains. Princeton University Press, Princeton.

van Kampen, N.G., 1992. Stochastic Processes in Physics and Chemistry. Elsevier, Amsterdam, San Diego, Oxford, London.

Wright, S., 1931. Evolution in Mendelian populations. Genetics 16, 97159.